Rectification in Tunneling Junctions: 2,2#-Bipyridyl-Terminated n -Alkanethiolates

Supporting Information

Rectification in Tunneling Junctions: 2,2'-Bipyridyl-terminated *n*-Alkanethiolates

Hyo Jae Yoon,[1,2] Kung-Ching Liao,[1] Matthew R. Lockett,[1] Sen Wai Kwok,[1] Mostafa Baghbanzadeh,[1] and George M. Whitesides[1,2,3]*

[1]Department of Chemistry and Chemical Biology, Harvard University, 12 Oxford Street, Cambridge, MA 02138 USA

[2]Department of Chemistry, Korea University, Seoul 136-701, Korea

[3]Wyss Institute for Biologically Inspired Engineering, Harvard University, 60 Oxford Street, Cambridge, MA 02138 USA

[4]Kavli Institute for Bionano Science & Technology, Harvard University, 29 Oxford Street, Cambridge MA 02138 USA

*Corresponding author e-mail: gwhitesides@gmwgroup.harvard.edu

Experimental Details

Materials: All reagents were purchased from Sigma-Aldrich, and used as supplied unless otherwise specified. All organic solvents were purchased from Sigma-Aldrich (dichloromethane, hexanes) or Fisher (200 proof ethanol), 18.5 MΩ water obtained from a Millipore Q-POD water purification system. 2-Phenyl-4-methylpyridine was prepared using a reported procedure.[1] For the contact electrode, high purity eutectic gallium-indium (EGaIn; >99.99%) was obtained from Sigma-Aldrich and used as supplied. All purified thiol derivatives were maintained under N_2 atmosphere and stored at < 4 °C.

Characterization: ^{1}H and $^{13}C\{^{1}H\}$ NMR spectra were recorded on a Bruker DPX 400 or a Varian INOVA 500 instrument using $CDCl_3$ as solvents and residual solvents as an internal standard. High-resolution mass spectrometry (HMRS) spectra were obtained on a Bruker microTOFII ESI LCMS instrument. X-ray photoelectron spectroscopy (XPS) spectra were obtained on a Thermo Scientific K-Alpha photoelectron spectrometer using Monochromatic Al K-α X-Ray radiation (1.49 kV, base pressure ~ 10^{-9} Torr). Survey spectra (1 eV resolution) were collected at a constant pass energy (158 eV) from a 400 μm diameter spot size. Peaks in the XPS spectra were fitted and integrated, after a Shirley background correction, using CasaXPS processing software.

Preparation of 2,2'-Bipyridyl-terminated *n*-Undecanethiol.

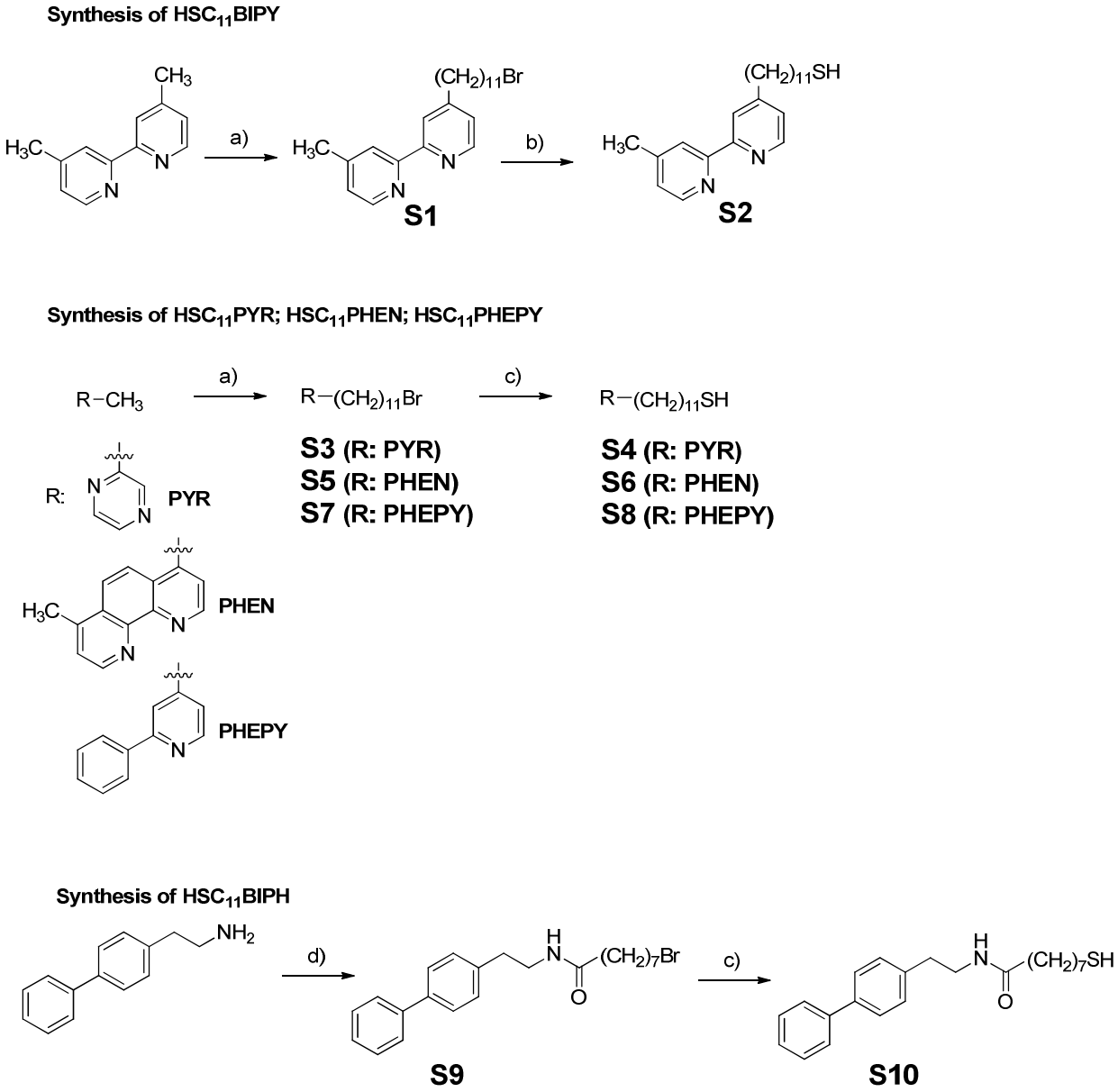

Scheme S1. Synthetic schemes for the preparation of thiol derivatives. a) 1,10-Dibromodecane, lithium diisopropylamide, THF, -78 ^{o}C. b) i) Potassium thioacetate, THF, reflux; ii) NaOH, EtOH, reflux. c) i) Thiourea, EtOH, reflux; ii) NaOH, EtOH, reflux. d) $ClC(O)(CH_2)_7Br$, triethylamine, CH_2Cl_2, rt.

Br-$(CH_2)_{11}$-(4'-methyl-2,2'-bipyridyl) (S1). To an oven-dried, 500-mL round-bottomed flask equipped with a magnetic stir bar and a rubber septum, 13.6 mL of 1.8 M lithium diisopropylamide (LDA) in heptanes/THF was added dropwise to a THF solution (150 mL) of 4,4'-dimethyl-2,2'-bipyridyl (23.3 mmol, 4.3 g) at -78 ^oC under N_2 atmosphere. The resulting solution was stirred at -78 ^oC for 1 h under N_2, and then warmed in an ice bath for 5 min. 1,10-Dibromodecane (119 mmol, 35.7 g) in 50 mL THF was added at once, the resulting solution stirred at 0 ^oC for 3h before water (50 mL) was added, and the pH of reaction solution adjusted to 7.0 with 1 M HCl. The reaction mixture was extracted with diethyl ether (3 × 100 mL), and the combined organic layers were concentrated *in vacuo*. The crude product was purified by silica-gel chromatography (eluent: 100% CH_2Cl_2 and then 100% ethyl acetate) to produce **S1** in 45% yield. ^1H NMR ($CDCl_3$, 400 MHz): δ 8.53 – 8.46 (m, 2H), 8.21 – 8.16 (m, 2H), 7.11 – 7.04 (m, 2H), 3.33 (t, 2H, J = 8 Hz), 2.63 (t, 2H, J = 8Hz), 2.37 (s, 3H), 1.85 – 1.72 (m, 2H), 1.69 – 1.57 (m, 2H), 1.42 – 1.15 (m, 14H). $^{13}C\{^1H\}$ NMR ($CDCl_3$, 125 MHz): δ 155.9, 153.1, 148.6, 148.3, 124.6, 123.9, 122.0, 121.33, 121.29, 35.4, 33.9, 32.7, 30.3, 29.33, 29.31, 29.26, 29.2, 29.1, 28.6, 28.0, 21.1. HRMS (m/z): $[M+Na]^+$ calcd. for $C_{22}H_{31}BrN_2Na$, 425.1563; found, 425.1578.

HS-$(CH_2)_{11}$-(4'-methyl-2,2'-bipyridyl) (S2). To a 25-mL round-bottomed flask equipped with a magnetic stir bar and a reflux condenser, a mixture of compound **S1** (1.54 mmol, 620 mg) and potassium thioacetate (1.54 mmol, 176 mg) in 20 mL of THF was refluxed for 24 h. The reaction solution was cooled to room temperature, concentrated *in vacuo*, and extracted with CH_2Cl_2 (3 × 10 mL). The combined organic layers were concentrated *in vacuo* to produce a thioester intermediate in quantitative yield. ^1H NMR ($CDCl_3$, 400 MHz): δ 8.61 – 8.51 (m, 2H), 8.28 (d, 2H, J = 8Hz), 7.17 (d, 2H, J = 4Hz), 2.85 (t, 2H, J = 8 Hz), 2.70 (t, 2H, J = 8Hz), 2.46 (s,

3H), 2.31 (s, 3H), 1.75 – 1.62 (m, 2H), 1.61 – 1.48 (m, 2H), 1.42 – 1.18 (m, 14H). $^{13}C\{^{1}H\}$ NMR ($CDCl_3$, 125 MHz): δ 195.9, 155.1, 153.6, 148.5, 148.4, 124.8, 124.1, 122.3, 121.63, 121.58, 35.5, 30.6, 30.3, 29.40, 29.37, 29.34, 29.29, 29.2, 29.1, 29.0, 28.7, 21.2. HRMS (m/z): $[M+Na]^+$ calcd for $C_{24}H_{34}N_2NaOS$, 421.2284; found, 421.2293. An ethanolic solution (10 ml) of NaOH (1.11 mmol, 45 mg) and the thioester (0.58 mmol, 230 mg) was prepared, degassed for 20 min with N_2, and refluxed for 2 h under N_2 atmosphere. The reaction solution was cooled to room temperature and extracted with CH_2Cl_2 (3 × 10 mL). The combined organic layers were concentrated *in vacuo*, and the crude product was purified by silica-gel column chromatography (eluent: 100% CH_2Cl_2 and then 100% ethyl acetate) to produce **S2** in 82% yield. ^{1}H NMR ($CDCl_3$, 400 MHz): δ 8.77 – 8.57 (m, 2H), 8.47 (d, 2H, J = 10Hz), 7.34 – 7.22 (m, 2H), 2.76 (t, 2H, J = 7.2 Hz), 2.54 – 2.46 (m, 5H), 1.79 – 1.66 (m, 2H), 1.64 – 1.53 (m, 2H), 1.43 – 1.16 (m, 15H). $^{13}C\{^{1}H\}$ NMR ($CDCl_3$, 125 MHz): δ 155.2, 153.4, 150.1, 147.8, 147.6, 146.5, 125.3, 124.6, 123.1, 122.3, 35.6, 34.0, 30.2, 29.42, 29.39, 29.3, 29.2, 29.1, 29.0, 28.3, 24.6, 21.4. HRMS (m/z): $[M+Na]^+$ calcd. for $C_{22}H_{32}N_2NaS$, 379.2178; found, 379.2183.

Br-$(CH_2)_{11}$-(2-pyrazinyl) (S3). To an oven-dried, 50-mL round-bottomed flask equipped with a magnetic stirbar, a rubber septum, and a balloon filled with argon, 8.3 mL of a 1.8 M solution of LDA in heptanes/THF was added to 5-mL of anhydrous THF. The solution was cooled to -78 °C, and stirred under argon for 30 min before 5 mL of a solution of 2-methyl pyrazine (10.8 mmol, 1.02 g) in anhydrous THF was added dropwise over a period of 15 – 20 min. The reaction mixture was stirred for an additional 3 h before a 5-mL solution of 1,10-dibromodecane (20.0 mmol, 6.00 g) in anhydrous THF was added dropwise over a period of 15 min. The reaction mixture warmed to room temperature overnight. An excess of solid NH_4Cl

was added to the reaction mixture, and the color of the reaction mixture changed from pink purple to orange yellow. The reaction mixture was subsequently filtered, and the filtrate concentrated *in vacuo* to yield a brown oil, which was purified by silica-gel column chromatography (eluent: 10% → 25% → 40% → 50% Et_2O in hexanes (v/v)) to yield product **S3** in 52% yield. ^{1}H NMR ($CDCl_3$, 400 MHz): δ 8.51 – 8.48 (m, 1H), 8.48 (d, 1H, J = 1.2 Hz), 8.42 (d, 1H, J = 2.4 Hz), 3.35 (t, 2H, J = 6.8 Hz), 2.82 (t, 2H, J = 7.6 Hz), 1.83 – 1.67 (m, 4H), 1.38 – 1.14 (m, 14H). ^{13}C{^{1}H} NMR ($CDCl_3$, 125 MHz): δ 157.7, 144.3, 143.2, 141.7, 35.1, 34.1, 32.7, 29.38, 29.35, 29.32, 29.26, 29.2, 28.7, 28.1. HRMS (m/z): $[M+H]^+$ calcd. for $C_{15}H_{26}BrN_2$, 313.1274; found, 313.1305.

HS-(CH_2)$_{11}$-(2-pyrazinyl) (S4). To a 25-mL round-bottomed flask equipped with a magnetic stirbar and a reflux condenser, 7.5 mL of thiourea (1.3 mmol, 99 mg) in anhydrous EtOH (7.5 mL) was added to 7.5 mL of 2-(11-bromoundecyl)pyrazine (**S4**) (1.2 mmol, 370 mg). The reaction mixture was refluxed under an atmosphere of N_2 for 24 h, and concentrated *in vacuo* to yield a beige solid. The beige solid was suspended in 10 mL of de-ionized water; the suspension was rapidly stirred, capped with a septum, and degassed with N_2. An aqueous solution of NaOH (1 M, 1.2 mL) was added to the suspension, and the reaction refluxed under N_2 for 4 h. The reaction mixture was cooled to room temperature under N_2, extracted with CH_2Cl_2 (2 × 20 mL), and the combined organic layers were dried over anhydrous $NaSO_4$, filtered, and concentrated *in vacuo* to yield a brown oil. The crude product was purified by silica-gel column chromatography (eluent: 10% → 20% EtOAc in CH_2Cl_2 (v/v); solvents were degassed by bubbling N_2 for 20 min) to produce **S4** in 73% yield. ^{1}H NMR ($CDCl_3$, 500 MHz): δ 8.42 – 8.41 (m, 1H), 8.39 (d, 1H, J = 2 Hz), 8.33 (d, 1H, J = 2.5 Hz), 2.74 (t, 2H, J = 8 Hz), 2.44 (q, 2H, J =

7.5 Hz), 1.70 – 1.64 (m, 2H), 1.55 – 1.49 (m, 2H), 1.30 – 1.16 (m, 15H). $^{13}C\{^{1}H\}$ NMR ($CDCl_3$, 125 MHz): δ 157.8, 144.3, 143.7, 141.8, 35.3, 33.8, 29.30, 29.28, 29.26, 29.21, 29.17, 29.1, 28.9, 28.2, 24.4. HRMS (m/z): $[M+H]^+$ calcd for $C_{15}H_{27}N_2S$, 267.1889; found, 267.1902.

Br-$(CH_2)_{11}$-(1,10-phenanthroline) (S5). Compound **S5** was synthesized following the synthetic procedure described for compound **S3**. ^{1}H NMR ($CDCl_3$, 500 MHz): δ 8.85 (d, 1H, J = 4.5 Hz), 8.80 (d, 1H, J = 4.5 Hz), 7.73 (d, 1H, J = 9.5 Hz), 7.67 (d, 1H, J = 9.0 Hz), 7.17 (d, 1H, J = 4.5 Hz), 7.15 (d, 1H, J = 4.0 Hz), 3.17 (t, 2H, J = 7.0 Hz), 2.83 (t, 2H, J = 8.0 Hz), 2.47 (s, 3H), 1.65 – 1.59 (m, 2H), 1.56 – 1.49 (m, 2H), 1.24 – 1.03 (m, 14H). $^{13}C\{^{1}H\}$ NMR ($CDCl_3$, 125 MHz): δ 149.2, 149.1, 148.0, 145.9, 145.7, 143.5, 127.0, 126.5, 123.3, 122.2, 121.34, 121.26, 33.5, 32.3, 31.8, 29.8, 29.0, 28.94, 28.93, 28.88, 28.85, 28.2, 27.6, 18.4. HRMS (m/z): $[M+Na]^+$ calcd for $C_{24}H_{31}BrN_2$, 449.1563; found, 449.1558.

HS-$(CH_2)_{11}$-(1,10-phenanthroline) (S6). Compound **S6** was synthesized following the synthetic procedure described for compound **S4**. ^{1}H NMR ($CDCl_3$, 400 MHz): δ 8.97 (d, 1H, J = 4.4 Hz), 8.93 (d, 1H, J = 4.4 Hz), 7.93 (d, 1H, J = 9.6 Hz), 7.88 (d, 1H, J = 9.6 Hz), 7.35 – 7.33 (m, 2H), 3.01 (t, 2H, J = 8.0 Hz), 2.66 (s, 3H), 2.43 (q, 2H, J = 7.2 Hz) 1.72 – 1.63 (m, 2H), 1.53 – 1.47 (m, 2H), 1.38 – 1.20 (m, 15H). $^{13}C\{^{1}H\}$ NMR ($CDCl_3$, 100 MHz): δ 149.7, 149.6, 148.7, 146.3, 146.1, 144.1, 127.6, 127.1, 123.9, 122.8, 121.9, 121.8, 34.0, 32.4, 30.3, 29.54, 29.46, 29.42, 29.38, 29.0, 28.3, 24.6, 18.9. HRMS (m/z): HRMS (m/z): $[M+H]^+$ calcd for $C_{24}H_{33}N_2S$, 381.2364; found, 381.2319.

Br-$(CH_2)_{11}$-(2-phenylpyridyl) (S7). Compound **S7** was synthesized following the synthetic procedure described for compound **S3**. ^{1}H NMR ($CDCl_3$, 300 MHz): δ 8.56 (d, 1H, J = 4.8 Hz), 8.00 – 7.67 (m, 2H), 7.54 – 7.39 (m, 4H), 7.05 (dd, 1H, J = 4.8 Hz, 1.2 Hz), 3.38 (d, 2H, J = 7.2 Hz), 2.65 (d, 2H, J = 7.5 Hz), 1.88 – 1.78 (m, 2H), 1.71 – 1.61 (m, 2H), 1.42 – 1.22 (m, 14H). ^{13}C{^{1}H} NMR ($CDCl_3$, 100 MHz): δ 157.2, 152.5, 149.3, 139.4, 128.7, 128.6, 126.8, 122.3, 120.7, 35.4, 33.9, 32.7, 30.3, 29.36, 29.35, 29.3, 29.1, 28.6, 28.0. HRMS (m/z): $[M+H]^+$ calcd for $C_{22}H_{30}BrN$, 388.1634; found, 388.1650.

HS-$(CH_2)_{11}$-(2-phenylpyridyl) (S8). Compound **S8** was synthesized following the synthetic procedure described for compound **S4**. ^{1}H NMR ($CDCl_3$, 400 MHz): δ 8.57 (d, 1H, J = 5.2 Hz), 7.99 (m, 2H), 7.54 – 7.40 (m, 4H), 7.07 – 7.05 (m, 1H), 2.66 (t, 2H, J = 7.6 Hz), 2.52 (q, 2H, J = 7.2 Hz), 1.71 – 1.56 (m, 4H), 1.41 – 1.21 (m, 15H). ^{13}C{^{1}H} NMR ($CDCl_3$, 100 MHz): δ 157.4, 152.5, 149.4, 139.6, 128.8, 128.7, 127.0, 122.4, 120.9, 35.5, 34.0, 30.4, 29.52, 29.48, 29.41, 29.2, 29.0, 28.4, 24.7. HRMS (m/z): $[M+H]^+$ calcd for $C_{22}H_{32}NS$, 342.2255; found, 342.2227.

HS-$(CH_2)_7$-CONH-$(CH_2)_2$-biphenyl (S10). Compounds **S9** and **S10** were synthesized following the synthetic procedure described in the literature.[2] **S9**: ^{1}H NMR ($CDCl_3$, 400 MHz): δ 7.59 – 7.53 (m, 4H), 7.46 – 7.42 (m, 2H), 7.36 – 7.32 (m, 1H), 7.28 – 7.26 (m, 2H), 5.54 (s, 1H), 3.56 (q, 2H, J = 6.4 Hz), 3.40 – 3.56 (m, 2H), 2.86 (t, 2H, J = 8.0 Hz), 2.14 (t, 2H, J = 7.2 Hz), 1.86 – 1.79 (m, 2H), 1.64 – 1.59 (m, 2H), 1.43 – 1.29 (m, 6H). ^{13}C{^{1}H} NMR ($CDCl_3$, 100 MHz): δ 166.0, 133.7, 132.5, 130.9, 122.2, 121.8, 120.3, 120.2, 119.9, 33.5, 29.7, 28.3, 26.9, 25.7, 22.0, 21.5, 20.9, 18.6. **S10**: ^{1}H NMR ($CDCl_3$, 400 MHz): δ 7.56 – 7.53 (m, 4H), 7.45 – 7.41

(m, 2H), 7.35 – 7.31 (m, 1H), 7.27 – 7.25 (m, 2H), 5.67 (s, 1H), 3.55 (q, 2H, J = 6.4 Hz), 2.86 (t, 2H, J = 6.4 Hz), 2.48 (q, 2H, J = 6.8 Hz), 2.13 (t, 2H, J = 7.6 Hz), 1.62 – 1.54 (m, 4H), 1.37 – 1.28 (m, 7H) 1.88 – 1.78 (m, 2H), 1.71 – 1.61 (m, 2H), 1.42 – 1.22 (m, 14H). $^{13}C\{^{1}H\}$ NMR ($CDCl_3$, 100 MHz): δ 173.0, 140.7, 139.3, 137.9, 129.1, 128.7, 127.2, 127.1, 126.9, 40.4, 36.6, 35.2, 33.8, 29.0, 28.7, 28.1, 25.6, 24.5. HRMS (m/z): $[M+H]^+$ calcd for $C_{22}H_{29}NOS$, 356.2043; found, 356.2040.

Preparation of SAMs. SAMs were prepared following the procedure reported previously.[2,3] Ultraflat, template-stripped silver substrates (Ag^{TS})[4,5] were submerged in an amber-colored vial containing a 3 mM ethanolic (200 proof; anhydrous) solution of an alkanethiol (e.g., HSC_{11}BIPY) and incubated under an N_2 atmosphere at room temperature for 3 h. The N_2 environment was intended to minimize corrosion of Ag surface, and oxidation of alkanethiol (to a disulfide or sulfonate). After incubation, the metal substrate was washed gently with 200 proof ethanol (3 × 1 mL), and residual solvent on surface was removed by gently blowing N_2.

Junction Formation and *J-V* Measurements. Values of $J(V)$ were measured using procedures described previously.[2] Junctions were formed by placing a conical microelectrode (~50 μm in diameter) of Ga_2O_3/EGaIn in conformal contact with the surface of the SAM using micromanipulator. We used unflattened[6,7] Ga_2O_3/EGaIn conical tips selected to avoid tips with visible asperities. During preparation of conical tips, the rupture of the EGaIn neck can create a whisker of Ga_2O_3 on the base of the conical tip (the detailed procedure to form conical tips is reported in literature[7,8]). We selected conical tips without an observable whisker for measurements of $J(V)$.

We measured the diameter of the contact area, and estimated the total area of contact by assuming the contact was uniform and circular. To confirm the EGaIn electrode was in contact with the SAM and formed a Ag^{TS}-SC_{11}BIPY//Ga_2O_3/EGaIn junction, we performed a single scan: 0V → +1.0V → 0V → -1.0V → 0V. If the junction was formed correctly, and did not short, we performed 20 more scans (i.e., each junction was used to collect 21 traces of $J(V)$).[6,7] A new Ga_2O_3/EGaIn electrode was prepared after every three junctions to minimize artifacts in the data that could arise from the adsorption of adventitious contaminants on the Ga_2O_3 surface, and to prevent the influence of unnecessary roughness at the tip of the Ga_2O_3/EGaIn electrode after multiple contacts with the SAM.

Table S1. Comparison of the rectification ratios and junction characteristics for molecular rectifiers claimed previously.

type of junction	Top Electrode	bottom electrode	molecular component	[a] $\lvert r^{\pm} \rvert$ (polarity)	$\sigma_{\log\lvert r \rvert}$	number of junctions	|V|	ref in the manuscript
SAM	Au	Au	[b] $S(CH_2)_{10}$-isoquinolium-dimethylaminobenzylidene/ $[Cu(II)phthalocyanine]_{0.25}^-$	3000 (-)	[o] -	-	1.0	ref. 14 (Ashwell, 2006)
SAM	[c] Ti/TiO_x	[d] PPF	[e] 4-nitrophenylazobenzene	600 (+)	-	67	2.0	ref. 6 (McCreery, 2003)
SAM	[f] Ga_2O_3/ EGaIn	[g] Ag^{TS}	$S(CH_2)_{11}Fc_2$	500 (-)	3.5	25	1.0	ref. 21 (Nijhuis, 2010)
SAM	PtIr	Au	[h] $S(CH_2)_3SO_3^-$/isoquinolium-dibutylaminobenzylidene	450 (-)	-	-	1.0	ref. 13 (Ashwell, 2006)
SAM/dendrimer multilayer	Ga_2O_3/ EGaIn	Ag^{TS}	[i] SR_1R_2-βCD/$X(Fc_2)_n$	170 (-)	1.9	20	2.0	ref. 19 (Wimbush, 2010)
SAM	Ga_2O_3/ EGaIn	Ag^{TS}	$S(CH_2)_{11}Fc$	150 (-)	2.1	31	1.0	ref. 20 (Nijhuis, 2013)
SAM	PtIr	Au	[j] $S(CH_2)_{10}$-quinolinium-dimethylaminonaphthalenyl-vinyl	50 – 150 (-)	-	1	1.0	ref. 10 (Ashwell, 2005)

LB	Au	Au	[k]$C_{16}H_{33}$Q-3CNQ	20 (+)	-	1	2.2	ref. 3 (Xu, 2001)
SAM	Au	Au	[l]$SC_{10}H_{21}$// D-π-A-$C_{10}H_{20}S$	18 (-)	-	-	1.0	ref. 8 (Ashwell, 2004)
LB	PtIr	Au	diblock co-oligomer (oligothiophene and oligothioazole)	18 (+)	-	-	1.0	ref. 4 (Ng, 2002)
LB	Hg-$SC_{16}H_{33}$	Au	[m]trinitrofluorene-σ-TTF	18 (-)	-	-	0.83	ref. 11 (Ho, 2005)
LB	Au	Au	[n]fullerene-terminated bis(triphenylamine)	17 (+)	-	-	5.4	ref. 12 (Honciuc, 2005)

[a] $r^+ = |J(+V)|/|J(-V)|$ and $r^- = |J(-V)|/|J(+V)|$; [b]$S(CH_2)_{10}$-5-(4-dimethylaminobenzylidene)-5,6,7,8-tetrahydroisoquinolinium/copper(II) phthalocyanine-3,4′,4″,4‴-tetrasulfonate; [c]Note: the authors later reported that rectification may depend both on the oxidized titanium electrode (Ti/TiO_x) and the molecular component (see reference 9 in the SI for detailed information).[9] [d]Pyrolyzed photoresist film;[e]Covalently attached monolayer of nitroazobenzene by reduction of 4-nitroazobenzene 4'-diazonium tetrafluoroborate; [f]Eutectic gallium-indium alloy (EGaIn) covered by a self-limiting Ga_2O_3 film (~0.7 nm); [g]Template-stripped silver substrate;[h]$S(CH_2)_3SO_3^-$/*N*-methyl-5-(4-dibutylaminobenzylidene)-5,6,7,8-tetrahydroisoquinolinium; [i]SR_1R_2-βCD: heptathioether functionalized βCD, $X(Fc_2)_n$: dendrimers functionalized with biferrocene termini; [j]1-(10-acetylsulfanyldecyl)-4-{2-(4-dimethylaminonaphthalen-1-yl)-vinyl}-quinolinium iodide; [k]Hexadecylquinolinium tricyanoquinodimethanide; [l]D-π-A-$C_{10}H_{20}S$: 1-(10-acetylsulfanyldecyl)-4-[2-(4-dimethylaminophenyl)vinyl]quinolinium iodide; [m]TTF: tetrathiafulvalene; [n]Fullerene-bis-[4-diphenylamino-4-(*N*-ethyl-*N*-2-ethyl)amino-1,4-diphenyl-1,3-butadiene] malonate; [o]not reported.

Table S2. Summary of the experimental procedures to prepare SAMs, prepare the EGaIn junctions, and measure tunneling current densities.

	Description of materials and experiments
Thiols (R-SH)	- Purified with silica gel column chromatography using degassed (by bubbling N_2 for at least 15 min) eluents. - Purified thiols were maintained under N_2 atmosphere and stored at <4 °C. - The purity of the alkanethiols were checked using ^{1}H NMR spectroscopy before use (note that thiols readily react in an O_2 atmosphere to give disulfides, sulfonates, and/or sulfonic acids).
Ag^{TS} substrates	- Prepared following the procedure reported previously.[4,5] - Freshly cleaved Ag^{TS} substrates were used directly after being rinsed with pure EtOH (3 × 1mL).
Solvent for preparation of SAM	- Anhydrous 200 proof EtOH was degassed by bubbling N_2 through the solution for ca. 15 min before adding the alkanethiol molecule.
Preparation of SAM	- Prepared following the procedure reported previously.[2,3] - The freshly cleaved and rinsed Ag^{TS} substrates were placed in 3 mM ethanol (anhydrous 200 proof; degassed) of the alkanethiol under N_2 atmosphere at room temperature for 3 h. - Rinsed with pure EtOH (3 × 1mL) after incubation.
Preparation of Ga_2O_3/EGaIn Tip	- Prepared following the procedure reported previously.[7] - Commercially available EGaIn (≥99.99%, Aldrich) was used. - Conical tips with no visibly observable whisker(s) were used.
Measurements	- Followed the "1-3-20" protocol reported previously.[7] - The sequence of applied voltage: 0V → +1.0V → 0V → -1.0V → 0V

Minor discussion

Background about Rectification

Measurements of rectification are self-referencing: the same junction is used to make measurements at opposite polarity.[3,10] Measuring the rectification of current, at applied voltages of different polarities, across the same region of a SAM, and across the same interfaces in the same junction without the need of reforming junctions between the SAM and the top electrode between measurements, eliminates or minimizes many of the uncontrolled variables associated with large-area junctions formed on SAMs.[3,10] These variables include: damage to the SAM when forming the top-electrode[11] or when making electrical measurements (e.g., by electromigration[12] of metal in the electrodes into filaments); variations in the contact area between the top-electrode and the organic insulator;[7] uncharacterized disorder in the structure of the SAM;[13] defects in (and the variable topography of) the metal substrate;[5] and contamination of the surface of the metal, SAM, or top-electrode by adventitious organic contaminants in the laboratory atmosphere. The self-referencing characteristic of rectification gives the distributions of rectification ratios that are often much narrower than distributions of current densities.

Understanding the basis of rectification in molecular junctions offers a particularly attractive opportunity to relate the electrical behavior (e.g., asymmetric *J-V* traces) of the junction to the structure of the molecules composing them. When examining a new rectifying junction, one first must establish that rectification is reproducible and statistically well-characterized before determining if the rectification is dominated by the SAM, or by another feature of the junction (e.g., redox chemistry occurring at the top or bottom electrodes, asymmetric metallic contacts at interfaces of the SAM with the top- and bottom-electrodes, or artifacts due to other processes such as electromigration[12]).

Rectifications in Previous Studies Shown in Table S1.

The ranges of *r* presented in Table S1 are higher than the values observed in non-rectifying aliphatic or oligo(phenylene) SAMs (r^+~1.0 – 3.0),[8] and cannot be rationalized easily by characteristics of the junction that are independent of the SAM (e.g., asymmetry in the work function between the two electrodes, or differences in the bonding or modes of contact at the interfaces between the SAM and the electrodes). A thorough analysis of rectification of many of these previously published systems is not presently possible because: their reproducibility is unproven, too few data are reported to differentiate mean values from outliers, or a molecular origin for rectification has not been demonstrated. We believe, however, that a number of these observations represent authentic rectification.

The Role of Backbone (Amide, -CONH- vs. Ethyl, -CH_2CH_2-) of SAM in Charge Tunneling Through EGaIn-based Tunneling Junctions.

We previously demonstrated that replacing -CH_2CH_2- with -CONH- in the backbone increases the synthetic accessibility of thiol derivatives with various terminal groups, and does not significantly influence $J(V)$.[2,6,14] Thus, for designing the backbone of thiol derivatives in this work, we used *n*-alkyl backbone with or without -CONH- in the middle.

Synthesis of Molecules, Preparation of SAMs, and Junction Measurements

All thiol derivatives were purified through silica-gel column chromatography using degassed (by bubbling N_2 through the solution for at least 15 min) eluents. The SI also summarizes the preparation of SAMs, fabrication of template-stripped silver (Ag^{TS}) substrates, preparation of Ga_2O_3/EGaIn conical tips, and assembly of junctions (Table S2). We formed

junctions using unflattened[15] Ga_2O_3/EGaIn conical tips selected to avoid tips with visible asperities (see the reference 15 for detailed information about selected unflattened conical tips). Flattened[7] and non-flattened conical tips[6,8,16] show statistically indistinguishable tunneling decay constants (β) and injection current densities (J_o) (for *n*-alkanethiolates on template-stripped silver substrates); we conclude the electrical behaviors of both tips are similar and do not affect junction measurements significantly, but have not explicitly studied the characteristics of the tip on rectification by BIPY.

We collected *J*-*V* traces over the range ±1.0V using procedures described in detail previously[2,3] for 27 Ag^{TS}/$S(CH_2)_{11}$BIPY//Ga_2O_3/EGaIn junctions on three different Ag^{TS} substrates. We collected 444 *J*-*V* traces (78% of the junctions did not short—that is, the yield of working junctions was 78%), and measured the current density (*J* in A/cm^2) at an applied bias of $V = \pm 1.0$ V). We compared tunneling currents at $V = \pm 1.0$V to study rectification for three reasons. i) We chose $V = \pm 1.0$V for comparisons with many rectifiers, reported previously, that were studied in $V = \pm 1.0$V (Table S1). In particular, these values of applied bias were used to study the well-characterized rectification of Fc-terminated SAMs. ii) We examined ranges of voltages, in ±0.1V increments, greater than ±1.0V and found that voltages greater than ±1.0V almost always resulted in shorting junctions (>95%). iii) Previous work by Wimbush *et al.*[17] showed that an applied bias of less than $|V|<1.0$V has no significant effect on $J(V)$ characteristic of applied junctions. Values of applied bias $|V|>1.0$V increased (by up to four orders of magnitude) the thickness of Ga_2O_3 film, and large polarization of these films led to significant changes in the electrical characteristics of EGaIn junctions.

Histogram of Rectification

Values of *r*, when measured in junctions with conical Ga_2O_3/EGaIn top electrodes, are usually approximately log-normally distributed.[3,18] We generated histograms of $\log|r^+|$ ($|r^+|$ at log scale), fit each histogram to a Gaussian curve, and obtained the mean ($\log|r^+|_{mean}$), the median ($\log|r^+|_{median}$), and the standard deviation ($\sigma_{\log|r|}$) of $\log|r^+|$.

XPS Analysis for Examining Formation of BIPY Complexes with Ga^{3+} or In^{3+}.

We designed an experiment using X-ray photoelectron spectroscopy (XPS) to explore the influence of formation (if it occurs) of complexes on the rectification we observed. We analyzed SAM surfaces using XPS before and after assembly of the junction. XPS is a technique with high sensitivity (up to ~0.1% atomic sensitivity);[19] XPS has been used to measure the atomic composition of monolayers of metal chelates,[20-22] and mixed monolayers.[20,22,23] Using XPS, we examined the composition of the region that has been contacted with the Ga_2O_3/EGaIn electrode. We have demonstrated previously that the effective area of contact between rough surfaces of Ga_2O_3 film and SAM is smaller (~10^{-4}) than the geometrical, nominal area of contact established by optical microscopy.[7] For detection of the formation of Ga^{3+} or In^{3+} complexes with BIPY, we wished to increase the area of contact between the Ga_2O_3 and SAM. Thus, in this particular experiment, we used, instead of conical tips,[6-8] a drop of Ga_2O_3/EGaIn; here, the Ga_2O_3 film is smoother and more compliant than the Ga_2O_3 film in a conical tip, and thus leads to larger (×10) effective area of contact between the Ga_2O_3 and the SAM. We also tried to increase the probability that the BIPY group would chelate a metal ion by making at least 20 successive contacts with a SAM on the same region.

The spectrum in Figure S2, after contact with the top electrode, contained signals corresponding to Ag, C, N, S, and O, but did not contain peaks corresponding to Ga (1115 eV for Ga 3d) or In (445 eV for In 3d). We attribute the trace amount of oxygen on the surface to molecules of water physisorbed on the surface, and not to an oxidized byproduct such as sulfonate, nor to gallium oxide transferred from the EGaIn electrode, because there was only a single sulfur 2p peak (~162 eV) corresponding to a thiolate, and gallium ions were not detected.

Figure S1. A plot of r^+ versus an applied bias V (V) for $Ag^{TS}SC_{11}BIPY//Ga_2O_3/EGain$ junctions. (Inset: a plot of $\log|r^+|$ versus V.)

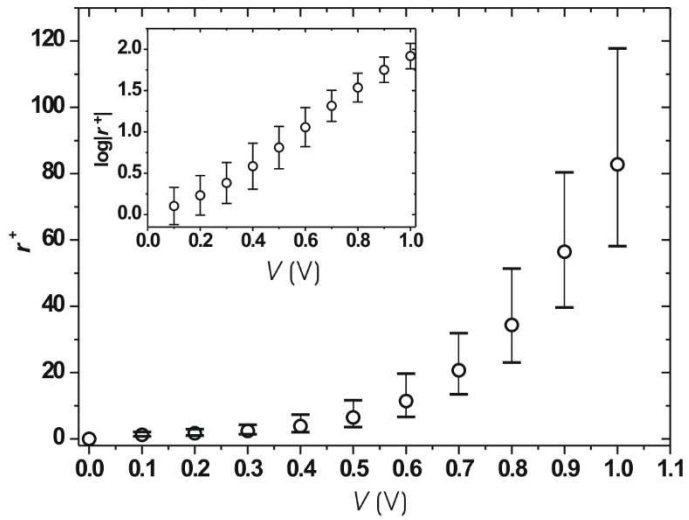

Figure S2. (a) Comparisons of XPS spectrum of a pristine Ag^{TS}/SC_{11}BIPY SAM (red line) with that of Ag^{TS}/SC_{11}BIPY SAM after 20 successive contacts with Ga_2O_3/EGaIn electrode (a black line). (b) High-resolution XPS spectra of Ga 3d and In 3d; these spectra present that there were no detectable signals for Ga 3d (~19 eV) or In 3d (~445 eV) in the SAM after repeated contact with the EGaIn electrode.

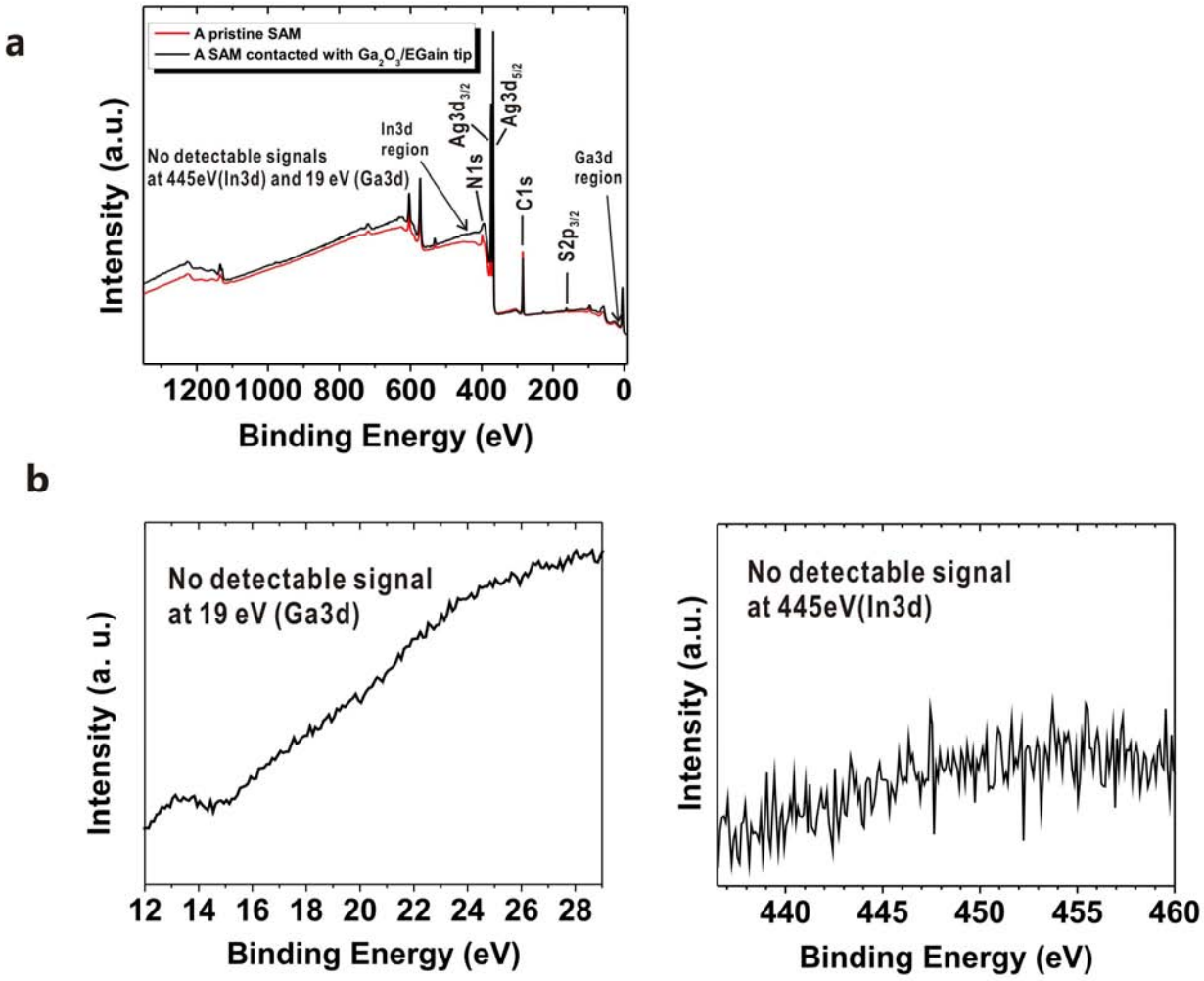

Figure S3. Histograms of $\log|r^+|$ at ±1.0V for SAMs terminated in different terminal groups (T in Figure 2) on a Ag^{TS} substrate.

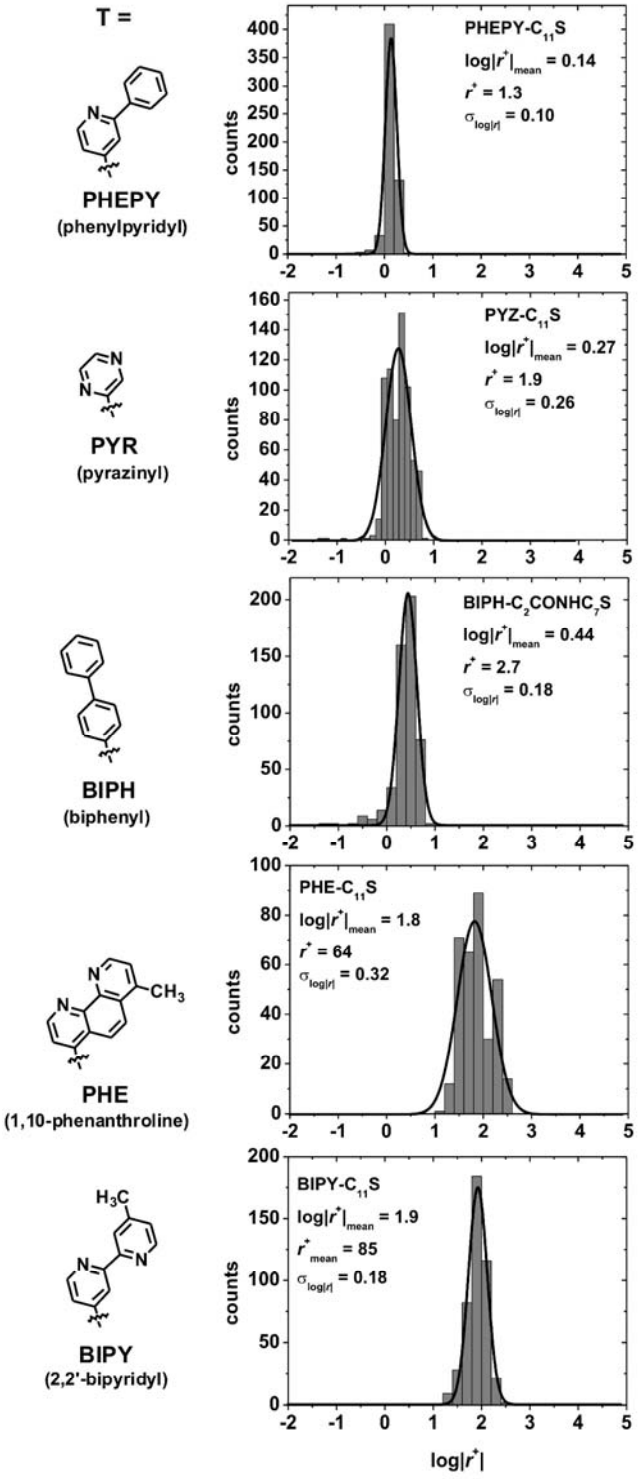

Figure S4. Histograms of current density at ±1.0V for different functional groups (T) in $Ag^{TS}S(CH_2)_{11}T//Ga_2O_3/EGaIn$ junctions.

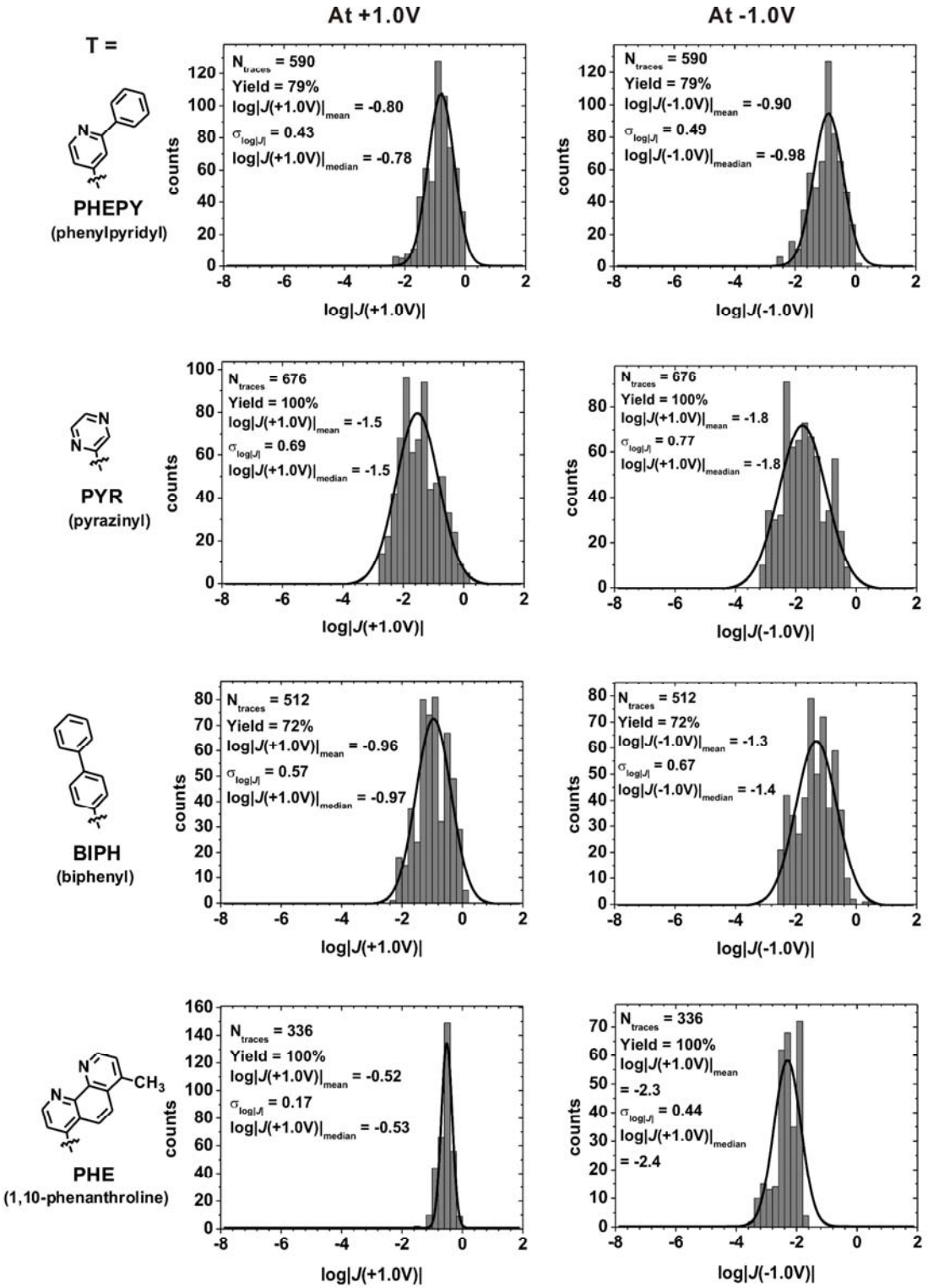

Figure S5. Molecular structures of some rectifiers described in Table S1. The structures of terminal groups were assumed to serve as rectifying moieties and used to calculate the molecular volume (V/Å^3; for structures in dashed line boxes) and width of tunneling barrier (d_{RM}/Å; for structures measured with arrows) corresponding to terminal group. Calculated values of d_{RM} are summarized in Table S3. References are based on those in the manuscript.

a. Ref. 14; Ashwell et al. 2006 (r^-_{obsd} = 3000)

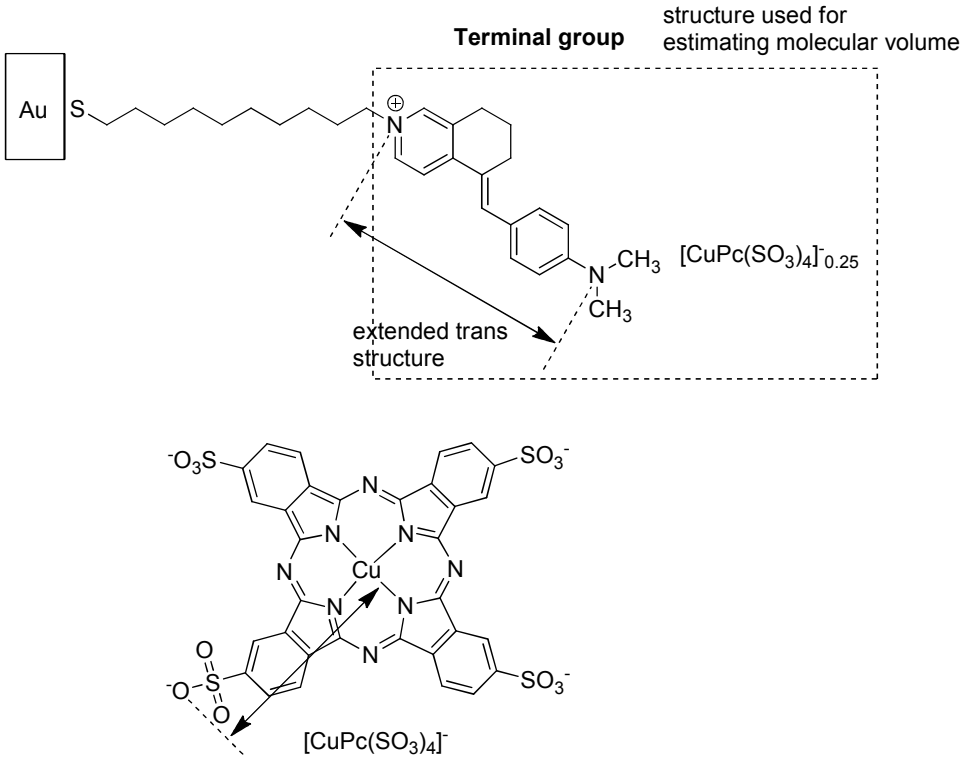

b. Ref. 6; McCreery et al. 2003 (r^+_{obsd} = 600)

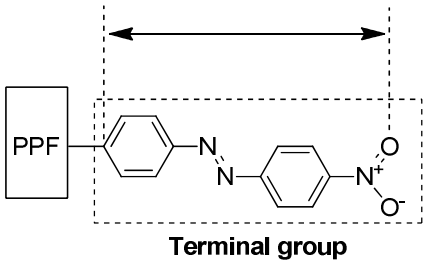

PPF: Pyrolyzed photoresist film

c. Ref. 21; Nihjuis et al. 2010 (r^{-}_{obsd} = 500)

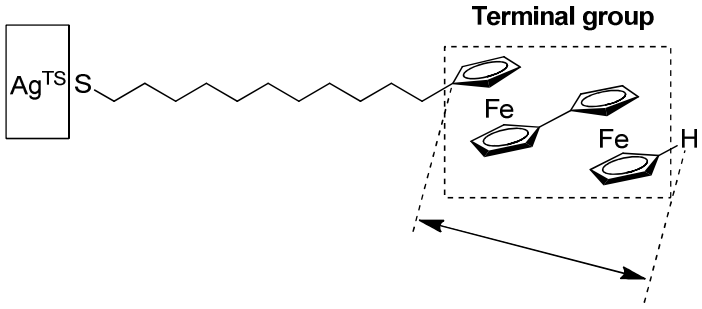

d. Ref. 13; Ashwell et al. 2006 (r^{-}_{obsd} = 450)

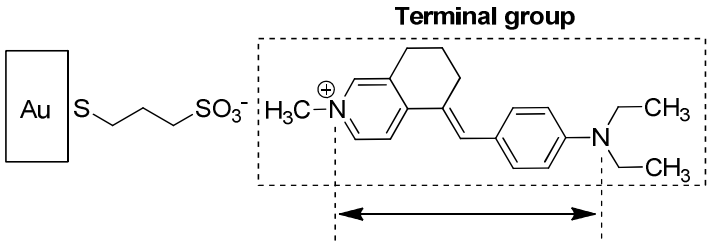

e. Ref. 20; Nijhuis et al. 2012 (r^{-}_{obsd} = 150)

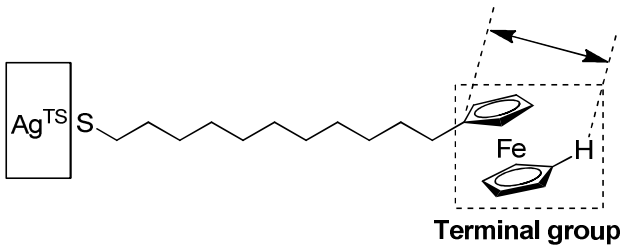

f. Ref. 10; Ashwell et al. 2005 (r^{-}_{obsd} = 50 - 150)

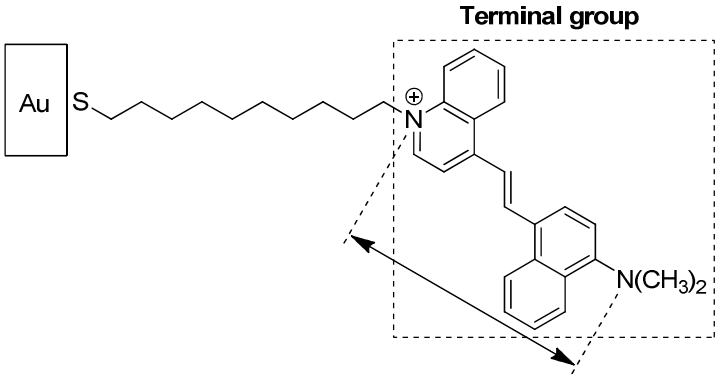

g. This work; $SC_{11}BIPY$ (r^{+}_{obsd} = 85)

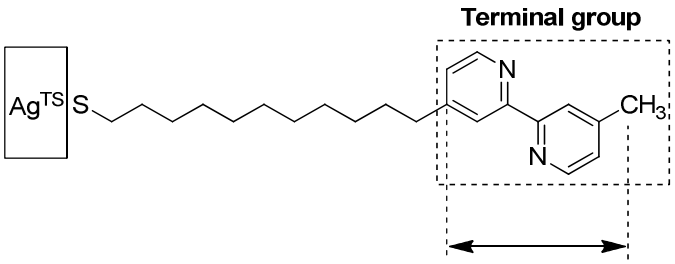

h. This work; $SC_{11}PHE$ (r^{+}_{obsd} = 67)

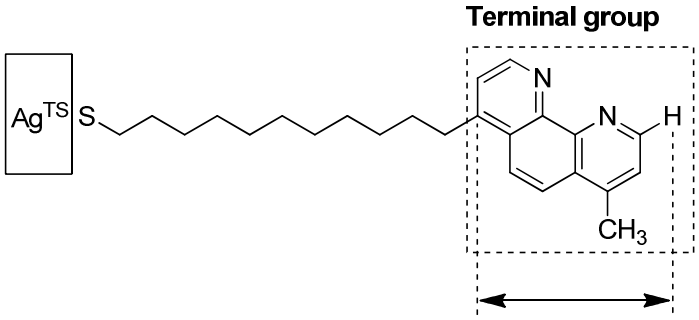

Table S3. Summary of calculations of d_{RM} based on two structural approximations: the terminal groups presented in Figure S5 as a sphere or an extended *trans* structure.

Structure of T group	Structure in Figure S5	V (Å^3)	d_{RM} (Å)	Rectification ratio (r)		
				Calcd[b] (β ~0.6Å^{-1})	Calcd[b] (β ~0.7Å^{-1})	Obsd (+/-)[c]
Spherical shape	a	267 (606)[a]	14.6	6390	27529	3000 (-)
	b	198	7.3	77	158	600 (+)
	c	371	8.9	210	512	500 (-)
	d	385	9.0	225	554	450 (-)
	e	192	7.2	73	150	150 (-)
	f	315	8.4	159	369	50-150 (-)
	g	164	6.8	59	116	85 (+)
	h	180	7.0	67	135	64 (+)
Extended *trans* structure	a	-	15.1	8608	38969	3000 (-)
	b	-	10.6	587	1700	600 (+)
	c	-	11.4	954	2994	500 (-)
	d	-	10.4	513	1452	450 (-)
	e	-	6.0	36	65	150 (-)
	f	-	10.3	470	1311	50-150 (-)
	g	-	7.2	75	154	85 (+)
	h	-	6.9	64	129	64 (+)

[a]The molecular volume for $[CuPc(SO_3)_4]^-$.
[b]Rectification ratios were calculated using Eq. 3 in the manuscript.
[c]The signs +/- indicate the polarity of rectification as defined in Eq. 1 and 2 in the manuscript.

References

(1) N. E. Shchepina, V. V. Avrorin, G. A. Badun, N. A. Bumagin, S. B. Lewis, S. N. Shurov, *Org. Med. Chem. Lett.* **2012**, *2*, 14.
(2) H. J. Yoon, N. D. Shapiro, K. M. Park, M. M. Thuo, S. Soh, G. M. Whitesides, *Angew. Chem., Int. Ed.* **2012**, *51*, 4658.
(3) C. A. Nijhuis, W. F. Reus, G. M. Whitesides, *J. Am. Chem. Soc.* **2009**, *131*, 17814.
(4) E. A. Weiss, R. C. Chiechi, G. K. Kaufman, J. K. Kriebel, Z. Li, M. Duati, M. A. Rampi, G. M. Whitesides, *J. Am. Chem. Soc.* **2007**, *129*, 4336.
(5) E. A. Weiss, G. K. Kaufman, J. K. Kriebel, Z. Li, R. Schalek, G. M. Whitesides, *Langmuir* **2007**, *23*, 9686.
(6) H. J. Yoon, C. M. Bowers, M. Baghbanzadeh, G. M. Whitesides, *J. Am. Chem. Soc.* **2014**, *136*, 16.
(7) F. C. Simeone, H. J. Yoon, M. M. Thuo, J. R. Barber, B. Smith, G. M. Whitesides, *J. Am. Chem. Soc.* **2013**, *135*, 18131.
(8) K.-C. Liao, H. J. Yoon, C. M. Bowers, F. C. Simeone, G. M. Whitesides, *Angew. Chem. Int. Ed.* **2014**, *53*, 3889.
(9) R. McCreery, J. Dieringer, A. O. Solak, B. Snyder, A. M. Nowak, W. R. McGovern, S. DuVall, *J. Am. Chem. Soc.* **2004**, *126*, 6200.
(10) C. A. Nijhuis, W. F. Reus, G. M. Whitesides, *J. Am. Chem. Soc.* **2010**, *132*, 18386.
(11) T.-W. Kim, G. Wang, H. Lee, T. Lee, *Nanotechnology* **2007**, *18*, 315204.
(12) T. Taychatanapat, K. I. Bolotin, F. Kuemmeth, D. C. Ralph, *Nano Lett.* **2007**, *7*, 652.
(13) J. C. Love, L. A. Estroff, J. K. Kriebel, R. G. Nuzzo, G. M. Whitesides, *Chem. Rev.* **2005**, *105*, 1103.
(14) M. M. Thuo, W. F. Reus, F. C. Simeone, C. Kim, M. D. Schulz, H. J. Yoon, G. M. Whitesides, *J. Am. Chem. Soc.* **2012**, *134*, 10876.
(15) J. R. Barber, H. J. Yoon, C. M. Bowers, M. M. Thuo, B. Breiten, D. M. Gooding, G. M. Whitesides, *Chem. Mater.* **2014**, *26*, 3938.
(16) C. M. Bowers, K.-C. Liao, H. J. Yoon, D. Rappoport, M. Baghbanzadeh, F. C. Simeone, G. M. Whitesides, *Nano Lett.* **2014**, *14*, 3521.
(17) K. S. Wimbush, R. M. Fratila, D. Wang, D. Qi, C. Liang, L. Yuan, N. Yakovlev, K. P. Loh, D. N. Reinhoudt, A. H. Velders, C. A. Nijhuis, *Nanoscale* **2014**, *6*, 11246.
(18) N. Nerngchamnong, L. Yuan, D. C. Qi, J. Li, D. Thompson, C. A. Nijhuis, *Nat. Nanotechnol.* **2013**, *8*, 113.
(19) C. C. Chusuei, D. W. Goodman In *Encyclopedia of Physical Science and Technology*; 3rd ed.; Meyers, R. A., Ed.; Elsevier: New York, 2004.
(20) G. B. Sigal, C. Bamdad, A. Barberis, J. Strominger, G. M. Whitesides, *Anal. Chem.* **1996**, *68*, 490.
(21) J. P. Folkers, C. B. Gorman, P. E. Laibinis, S. Buchholz, G. M. Whitesides, *Langmuir* **1995**, *11*, 813.
(22) T. Nakaji-Hirabayashi, K. Kato, Y. Arima, H. Iwata, *Biomaterials* **2007**, *28*, 3517.
(23) K. E. Nelson, L. Gamble, L. S. Jung, M. S. Boeckl, E. Naeemi, S. L. Golledge, T. Sasaki, D. G. Castner, C. T. Campbell, P. S. Stayton, *Langmuir* **2001**, *17*, 2807.